Density functional theory studies on the potential energy surface and hyperpolarizability of polyamidoamide dendrimer

ARTICLE *in* CHEMICAL PHYSICS LETTERS · SEPTEMBER 2002

Impact Factor: 1.9 · DOI: 10.1016/S0009-2614(02)01213-7

6 AUTHORS, INCLUDING:

Kechen Wu
Chinese Academy of Sciences
154 PUBLICATIONS **1,486** CITATIONS
SEE PROFILE

Chao-Yong Mang
Dali University
49 PUBLICATIONS **168** CITATIONS
SEE PROFILE

9 September 2002

Chemical Physics Letters 363 (2002) 343–348

CHEMICAL PHYSICS LETTERS

www.elsevier.com/locate/cplett

Density functional theory studies on the potential energy surface and hyperpolarizability of polyamidoamide dendrimer

Chensheng Lin, Kechen Wu *, Rongjian Sa, Chaoyong Mang, Ping Liu, Botao Zhuang

State Key Laboratory of Structural Chemistry, Fujian Institute of Research on the Structure of Matter, Chinese Academy of Sciences, Fuzhou, Fujian 350002, China

Received 19 April 2002; in final form 17 July 2002

Abstract

The potential energy surface and hyperpolarizabilities of the core (G0) and the first generation (G1) of polyamidoamide (PAMAM) dendrimer are studied by using the density functional theory with both the basis sets optimized for B3LYP method and the medium-size polarized GTO/CGTO basis sets for calculations of molecular polarizability. The inversion barrier of G1 is 941.4 cm^{-1}, which indicates that the back folding of the branches is very easy for this dendrimer construction. It is found that in most cases, the first hyperpolarizabilities β of G1 will increased when the molecular structure is distorted from its equilibrium arrangement. These results provide structural guidelines for the optimization of β by means of changing the dendrimer shape in different solvents.

1. Introduction

In recent years, dendrimers have attracted more and more researchers attention [1–5]. The chemistry of these materials has matured to the level at which a large number of compositionally different families have been successfully synthesized and some are already commercially available. However, the potential applications, particularly in materials science and engineering, will not be realized before the physical properties are deeply studied. The dendrimer intramolecular morphology is one of the most intriguing but yet unresolved issues. Undoubtedly, this property will directly predetermine many macroscopic features and potential uses, for example as advanced catalysts, agents in molecular encapsulation, adhesive modifiers and nonlinear optical materials.

Dendrimers are regularly branched, tree-like macromolecules with a branch point at each monomer unit. The repeated units emanated from either a single central atom or atomic group, referred to as the core. The well-known dendrimer is polyamidoamide (PAMAM, shown in Fig. 1). In a geometrical context, this tree-like structure may be viewed as triads of symmetrical trees rooted to a

* Corresponding author. Fax: +86-591-371-4946.
E-mail address: wkc@ms.fjirsm.ac.cn (K. Wu).

0009-2614/02/$ - see front matter
PII: S0009-2614(02)01213-7

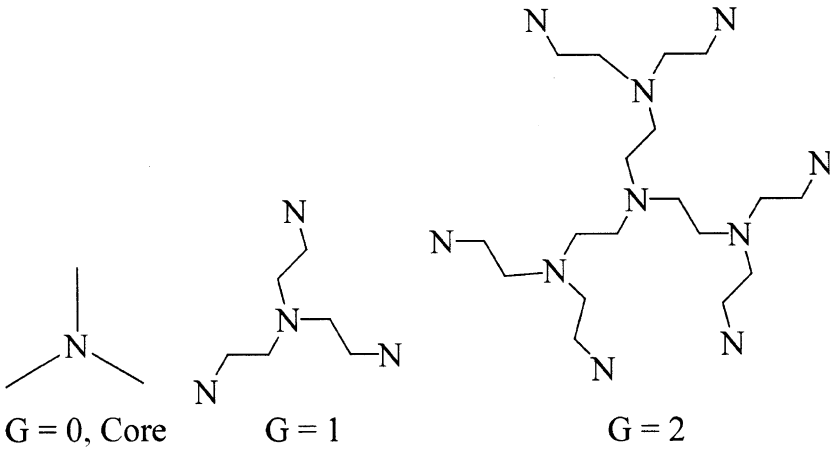

Fig. 1. Schematic diagrams of PAMAM dendrimer, showing generation number.

common initiator core. Such a dendrimer consists of a core, with connectivity to vertices through branch segments which expand symmetrically according to a geometric progression to produce generations containing predictable numbers of vertices and edges. Since the branch numbers of the dendrimers is exponential of the generation number and grow much more rapidly than the available volume, the structure saturates at a given generation number, beyond which it is impossible to grow the dendrimer to completion.

Experimental determination of exact shapes of dendrimers has turned out to be difficult, primarily because most of the commonly used techniques reach their reliability limits in the size domain of lower dendrimer generations. A few theoretical studies on PAMAM, mainly with Monte Carlo method and mean-field model, have now appeared [6–9]. There are some qualitative conclusions of PAMAM geometry structure, such as the back folding behavior of end groups, the hardness of the molecule increasing with generation, and the fully developed dendrimers do not engage in interdendrimer interaction. In this Letter, we report a first-principle based DFT calculation to explore the potential energy surface of the first PAMAM generation and draw quantitative conclusions of the inversion, wag and torsion barrier. The relationships between the dendrimer morphology and its nonlinear optical responses are also studied.

2. Computational method

The DFT method was used to carry out the calculations of geometry optimization and the potential energy surface (PES). The exchange-correlation energy functional used in this work was the hybrid method with Becke's exchange [10] and the correlation of Lee, Yang and Parr [11] denoted as B3LYP. In the structure optimized calculations, we used the DZVP orbital basis set, for N and C we used (621/41/1) and for H (4/1). This basis set is optimized for DFT calculations [12], and it is a approximately equivalent to a double-zeta valence plus polarization basis set.

The numerical differentiation of energy technology was used to calculate the molecular hyperpolarizability. The static first hyperpolarizabilities β tensors were calculated by using the finite-field method (FF method) at the time independent DFT level. The relative large polarizability consist basis sets (52111/411/22 for C and N, 411/22 for H) recommended by Sadlej [13] were used. All calculations were carried out by using the GAUSSIAN 98 program package [14].

3. Results and discussion

The core of PAMAM is molecule NH_3, which has been intensively studied by experimental

[15–17] and theoretical [18–20] methods. For the sake of comparison, we calculated the inversion barrier of NH_3 by using the DFT method and the QCISD//6-311++G** method as showed in Fig. 2. The molecular structure is optimized at each α angle, which is the angle between N–H bond and the C_3 symmetry axis of NH_3. The equilibrium structure of DFT optimized is $R_{N-H} = 1.018$ Å, $\alpha = 22°13'$, whereas the experimental value was $R_{N-H} = 1.011 \pm 0.004$ Å, $\alpha = 22°12' \pm 13'$. The inversion barrier of DFT calculations is 2013.28 cm^{-1}, while the result of QCISD is 1914.39 cm^{-1}. Both results are in good agreement with the experimental values, 2020 ± 12 cm^{-1} [15].

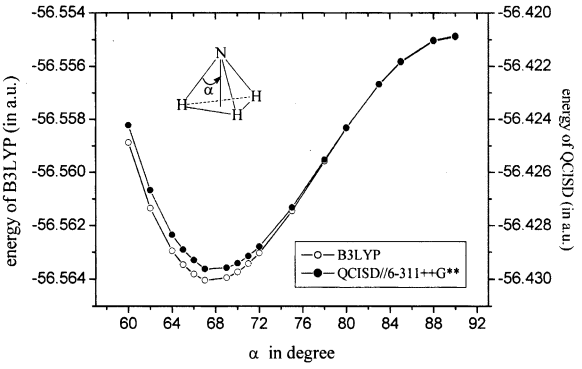

Fig. 2. Calculated energies along the ammonia inversion coordinate. α is the angle between the N–H bond and the C_3 symmetry axis of NH_3.

Although it is true that the B3LYP function was constructed with data from molecules in their equilibrium configuration, we see that, at least in this case, it works well out of equilibrium.

The static first hyperpolarizability ($\beta_{//}$) of NH_3 of DFT calculated result is 33.54 a.u., which is in the range of most literature values (Table 1). However, there are significant inconsistencies from a theory to another due to some reasons. The first is the basis set problem. Apart from the FF method, the prediction of hyperpolarizabilities depends upon products of matrix elements of the electron position operator, $\hat{r}$. Consequently, unlike the molecule's energy, which primarily depends upon inverse powers of $\hat{r}$, the study of hyperpolarizabilities must allow for an adequate description of the more diffuse regions of the molecule's wave function. We noted that Guan et al. obtained LDA estimates for β_{zzz} ranging from 5.76 to 82.6 a.u. with various basis sets [27]. In our calculation, the DZVP basis set draws a value of 22.58 a.u. for $\beta_{//}$, which is seemed too small compared with other high level theoretical results. The second factor is the electron correlation effect. It is important to include the accurate electron correlation to obtain reliable values. For the small molecules, correlation could change the predicted static hyperpolarizabilities β to a factor of 2. In addition to the electronic response, there exists vibrational contribution to the hyperpolarizabilities, especially in the case of second

Table 1
The components of first hyperpolarizabilities of NH_3 molecule (in a.u.)

	TDHF[a]	CCSD(T)[b]	SDQ-MP4[c]	CPHF[d]	LDA[e]	LB94[f]	B3LYP[g]
β_{zzz}	−6.98	−39.6	34.02	−7.758	−64.4	−30.7	32.69
β_{zxx}	−6.728	−8.8	8.38	−6.840	−14.3	−10.0	11.61
β_{yxx}	9.410			−8.930	8.0		
$\beta_{//}$[h]	12.26	34.3	30.47	12.863	55.6	30.5	33.54

[a] Ref. [21], z is taken as the C_3-axis.
[b] Ref. [22], z is the principal axis of the molecule.
[c] Ref. [23], z is the C_3-axis, one hydrogen atom on the xz-plane and nitrogen along the positive z-axis.
[d] Ref. [24], z axis $\equiv C_3$, yz-plane $\equiv \sigma_1$.
[e] Ref. [25].
[f] Ref. [26].
[g] Present work. z is the principal axis of the molecule, the H atoms are located in the $-z$ direction, $xz \equiv \sigma_1$.
[h] $\beta_{//} = (3/5)(\beta_{zzz} + 2\beta_{zxx})$, since $\beta_{//}$ is usually defined as the projection of the first hyperpolarizability on the dipole moment, the value listed here is absolute for the convenience of comparison.

hyperpolarizabilities γ [28,29]. The last factor is that there is some confusion and several errors arising from different systems of definition and notation, obscure conventions for signs adopted in different papers, unspecified coordinate reference, etc. Furthermore, for the sake of comparison with the experimental values, the frequency dependence of the first hyperpolarizability needs to be considered. Aiga and Maroulis had reported [22,23], if the frequency dependence effects were took into account, the CCSD(T) and SDQ-MP4+T4 results of the static $\beta_{//}$ values, about 34.0 a.u., would give a reliable estimation to the dc-electric-field induced optical second-harmonic generation (ESHG) experimental value, 48.4 a.u. [30]. Our calculated results are not only in good agreement with the absolute value of the first hyperpolarizabilities, but also could draw the same trends of the β values dependence on the molecular geometry of the most reliable CCSD(T) calculations (see Fig. 3). It should be mentioned that the DFT schemes based on conventional exchange-correlation functions would not always give the comparable results of the ab initio/post-SCF such as MP2, especially for the case of conjugated systems when the polarization is due to donor/acceptor substitution, it drew a nearly catastrophic behavior of β with respect to increasing the chain length [30]. However, this problem has been resolved on someway with the latest research [31].

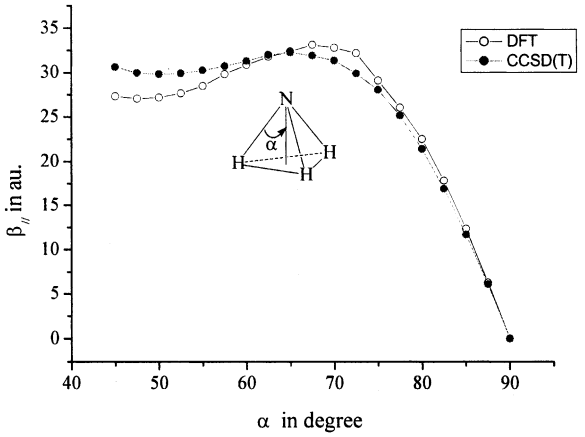

Fig. 3. The static first hyperpolarizability of NH_3 with CCSD(T) and DFT method.

Fig. 3 showed that the $\beta_{//}$ had its largest values at the optimized structure. In the inversion motion of the molecule, the energy reached its maximum value while $\beta_{//}$ decrease to its minimum value at point $\alpha = 90°$. This is because if $\alpha = 90°$, the symmetry would be much higher than C_s, which will lead the hyperpolarizability component β_{zzz} and β_{zxx} to vanish.

Compared with NH_3, the PES of G1 is very complicated because of the rotation of C–N and C–C bonds. As a reasonable simplification, we calculated the following three PES: (1) the inversion mode like the NH_3 molecule; (2) a C–N bond rotates around the main axis of the molecule while the other two C–N bonds keep in their origin positions, denoted as wag mode; (3) a C–N bond inverts relative to the main axis while the other two C–N bonds hold still, denoted as twist mode. These three behaviors represented most of the distortion of the dendrimer. The molecular structure is optimized at each angle of the distortion (see Fig. 4).

The inversion barrier of G1 PAMAM is 941.4 cm^{-1} (Fig. 5), which is much lower than that of the NH_3 molecule. The low energy barrier indicated that the fraction of the branches is very easy to fold back. This result is consistent with other theoretical results [32]. Unlike the NH_3 molecule, G1 has not the C_s symmetry when α is equal to 90°. At this point, the molecular $\beta_{//}$ is larger than that of its optimization geometry. For the molecular G1, the evolution of $\beta_{//}$ as a function of the angle α is more complicated than the case of NH_3: in the inversion mode, $\beta_{//}$ first increases with the increasing magnitude of energy, peaks at the point near 84°, then decreases. In the wag mode, $\beta_{//}$ has its minimum values around the optimized structure, and then increases with the energy increasing. In the twist mode, $\beta_{//}$ increases with the increasing of α degree from 40° to 100°, which is not the same trend of the molecular energy.

As a reasonable estimation, the traditional two-level model $\beta_{zzz}^{\text{model}}$ [33,34] can be used to explain the geometry dependence of β. $\beta_{zzz}^{\text{model}}$ only takes into account the ground state $|g\rangle$ and the first excited state $|e\rangle$

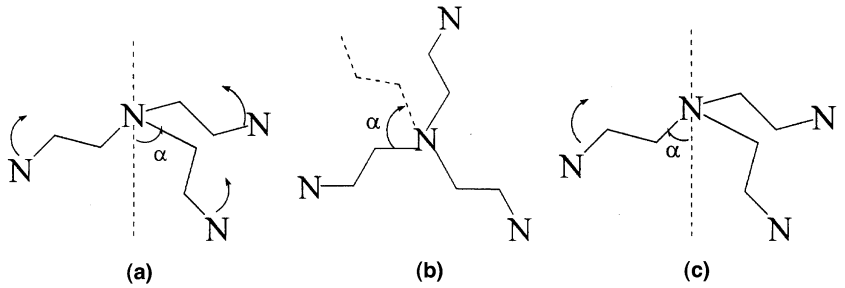

Fig. 4. The three modes of PES, (a) inversion mode, (b) wag mode, (c) twist mode.

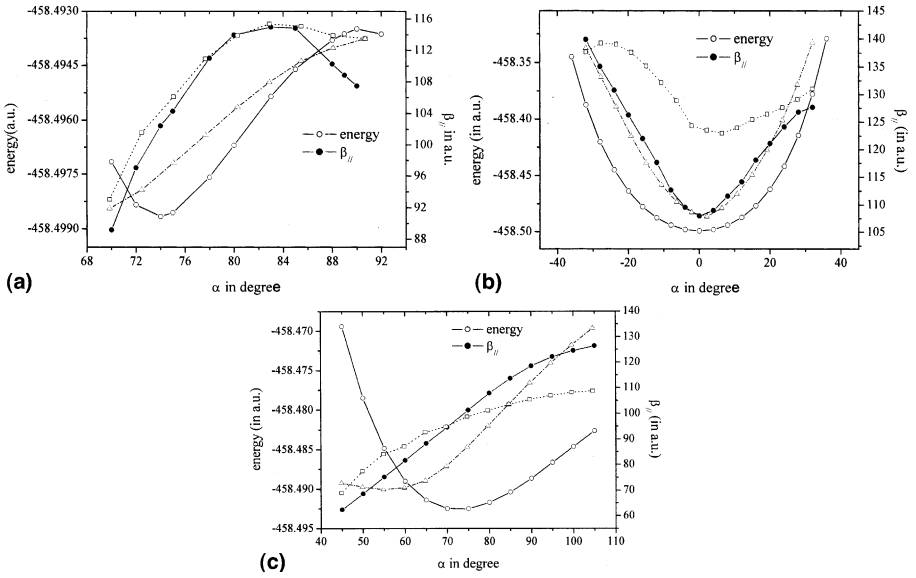

Fig. 5. The first hyperpolarizability and the inversion barrier (a), the wag mode PES (b) and the twist mode PES (c) of G1 varied with the α angle. The $1/E_{ge}$ (dash dot line) and Δu_z (dot line) is also plotted.

$$\beta_{zzz}^{\text{model}} = 6\frac{\langle g|u_z|e\rangle(\langle e|u_z|e\rangle - \langle g|u_z|g\rangle)\langle e|u_z|g\rangle}{E_{ge}^2} = 6\frac{M_{ge}^2\Delta u}{E_{ge}^2},$$

where Δu is the difference between the dipole moments in the first excited state and the ground state, E_{ge} is the energy difference of $E_g - E_e$ and M_{ge} is the transition dipole moment between the ground state and the first excited state. We calculate the values of Δu and E_{ge} in each point by using the TD–DFT method.

Fig. 5 showed that the evolution of $1/E_{ge}$ as a function of α is similar to that of molecular energy E. In the inversion mode, the $1/E_{ge}$ increases with the α angle increases from the optimized point 72° to 90°. However, both $1/E_{ge}$ and Δu remain decrease when α decreases from the optimized point, which is the same as $\beta_{//}$. In the wag mode, the values of Δu, $1/E_{ge}$, $\beta_{//}$ and E reach their minimum near the optimized structure point. While in the twist mode, both Δu and $1/E_{ge}$ increase with α values. In the two-level mode, β_{zzz} is fully determined by the following three factors: Δu, E_{ge} and M_{ge}. Unfortunately, the M_{ge} values from TD–DFT

calculations are too small to show the trends. For example, when α increases from $-20°$ to $0°$ by step size of $4°$, the values of M_{ge} $(\times 10^4)$ in wag mode are 44, 46, 47, 47, 46, 43, 41, respectively. The underestimation of M_{ge} lead the absolute value of β_{zzz}^{model} to be incomparable with $\beta_{//}$. In spite of this, the trends of Δu and E_{ge} have already revealed the origin of the β_{zzz}, and their behaviors are critical to $\beta_{//}$.

4. Conclusion

We drew the following conclusions from the DFT calculations on PAMAM. (1) The inversion energy barrier of G1 is very low, which indicated that the easy folding back of the branches. (2) The first hyperpolarizabilities of G1 vary as its structure varying. In all cases, the β value of equilibrium structure is not the largest one, and the distortion of the structure will lead to the increase of β value in some cases. As most theoretical studies focus on the molecular second-order nonlinear optical properties of its optimized structure, we show here the nonlinear optical properties of the distorted structures, which is the general condition of dendrimer in the solvent.

Acknowledgements

The work is supported by the National Science Foundation of China (NSFC, Grant No: 69978021, 20173064).

References

[1] A.W. Bosman, H.M. Janssen, E.W. Meijer, Chem. Rev. 99 (1999) 1665.
[2] G.R. Newkome, E. He, C.N. Moorefield, Chem. Rev. 99 (1999) 1689.
[3] D.A. Tomalia, A.M. Naylor, W.A. Goddard III, Angew. Chem. Int. Ed. Engl. 29 (1990) 138.
[4] S. Hecht, J.M.J. Frechet, Angew. Chem. Int. Ed. 40 (2001) 74.
[5] V.D. Kleiman, J.S. Melinger, D. McMorrow, J. Phys. Chem. B 105 (2001) 5595.
[6] M.L. Mansfield, L.I. Klushin, Macromolecules 26 (1993) 4262.
[7] L. Lue, Macromolecules 33 (2000) 2266.
[8] J.G. Jang, S.T. Noh, Y.C. Bae, J. Phys. Chem. A 104 (2000) 7404.
[9] S. Uppuluri, S.E. Keinath, D.A. Tomalia, P.R. Dvornic, Macromolecules 31 (1998) 4498.
[10] A.D. Becke, Phys. Rev. A 38 (1988) 3098.
[11] C. Lee, W. Yang, R.G. Parr, Phys. Rev. B 37 (1988) 785.
[12] N. Godbout, D.R. Salahub, J. Andzelm, E. Wimmer, Can. J. Chem. 70 (1992) 560.
[13] A.J. Sadlej, Theor. Chim. Acta 79 (1991) 123.
[14] M.J. Frisch, et al., GAUSSIAN, Pittsburgh, PA, 1998.
[15] J.D. Swalen, J.A. Ibers, J. Chem. Phys. 36 (1962) 1914.
[16] S. Urban, J. Mol. Spectrosc. 88 (1981) 24.
[17] V. Spirko, J. Mol. Spectrosc. 101 (1983) 30.
[18] G. Campoy, A. Palma, L. Sandoval, Int. J. Quantum Chem. Symp. 23 (1989) 355.
[19] D.J. Rush, K.B. Wiberg, J. Phys. Chem. 101 (1997) 3143.
[20] N. Aquino, G. Campoy, H. Yee-Madeira, Chem. Phys. Lett. 296 (1998) 111.
[21] F. Aiga, R. Itoh, Chem. Phys. Lett. 251 (1996) 372.
[22] H. Sekino, R.J. Bartlett, J. Chem. Phys. 98 (1993) 3022.
[23] G. Maroulis, Chem. Phys. Lett. 195 (1992) 85.
[24] P. Lazzeretti, R. Zanasi, J. Chem. Phys. 74 (1981) 5216.
[25] R.M. Dickson, A.D. Becke, J. Phys. Chem. 100 (1996) 16105.
[26] S.J.A. Van Gisbergen, J.G. Snijders, E.J. Baerends, J. Chem. Phys. 109 (1998) 10657.
[27] J.G. Guan, P. Duffy, J.T. Carter, D.P. Chong, K.C. Casida, M.E. Casida, M. Wrinn, J. Chem. Phys. 98 (1993) 4753.
[28] B. Champagne, Chem. Phys. Lett. 261 (1996) 57.
[29] B. Kirtman, B. Champagne, Int. Rev. Phys. Chem. 16 (1997) 389.
[30] B. Champagne, E.A. Perpete, D. Jacquemin, S.J.A. van Gisbergen, E.J. Baerends, C. Soubra-Ghaoui, K.A. Robins, B. Kirtman, J. Phys. Chem. A 104 (2000) 4755.
[31] M. van Faassen, P.L. de Boeij, R. van Leeuwen, J.A. Berger, J.G. Snijders, Phys. Rev. Lett. 88 (2002) 186401.
[32] A. Frischknecht, G.H. Fredrickson, Macromolecules 32 (1999) 6831.
[33] J.L. Oudar, D.S. Chemla, J. Chem. Phys. 66 (1977) 2664.
[34] J.L. Oudar, J. Chem. Phys. 67 (1977) 446.